JOINT INSTITUTE FOR NUCLEAR RESEARCH

*Dzhelepov Laboratory of Nuclear Problems*

# FINAL REPORT ON THE INTEREST PROGRAMME

## *Radiation effects study on MWCNT exposed to electron beam and gamma rays using the Raman Spectroscopy*


**Supervisor:**
Dr. Antonio Leyva Fabelo

**Student:**
Ștefana Ana Maria, Romania
„Babeș-Bolyai" University of Cluj-Napoca


**Participation period:**
September 27 – November 5, Wave 5

Dubna, 2021

# Abstract

The current study presents the changes that appear in the multi-walled carbon nanotubes, after they were irradiated with $^{60}$Co gamma rays and 20 MeV electrons. The nanotubes were analysed using Raman Spectroscopy, both before and after irradiation. The measured spectra underwent the process of deconvolution with OriginPro v9, applying the Voigt function. The analysis of the decomposed peaks revealed structural changes in the irradiated samples. The two types of radiation have a positive influence on the structure of the target MWCNTs, favouring the increase in the crystallinity of the material as a result of the reduction of the defect. Additionally, evidence was found that electron irradiation has an exfoliating effect on the multilayer structure of the samples.

# Introduction

Raman Spectroscopy is a spectroscopic technique, used for the study of low frequency modes [1]. It is based on inelastic scattering, or Raman scattering, of monochromatic light, usually a laser in the visible light range, near-infrared or near-ultraviolet. The laser light interacts with the phonons and other excitations in the system, causing the energy of the laser's photons to shift upwards or downwards. The energy shift gives information about the vibrational modes in the system, which in turn are going to be related to the characteristics of the white crystalline structure. A modification of the crystalline structure, such as the appearance of defects or the modification of its concentration, should lead to the manifestation of changes in the vibrational modes Raman [2].

Carbon nanotubes are a hot topic of today's reasearch, due to their particular mechanical and electrical properties, such as stiffness or conductivity. Multi-walled nanotubes (MWNTs) consist of multiple rolled layers (concentric tubes) of graphene. There are two models that can be used to describe the structures of multi-walled nanotubes. In the Russian Doll model, sheets of graphite are arranged in concentric cylinders, e.g., a (0,8) single-walled nanotube (SWNT) within a larger (0,17) single-walled nanotube. In the Parchment model, a single sheet of graphite is rolled in around itself, resembling a scroll of parchment or a rolled newspaper. The interlayer distance in multi-walled nanotubes is close to the distance between graphene layers in graphite, approximately 3.4 Å [3].

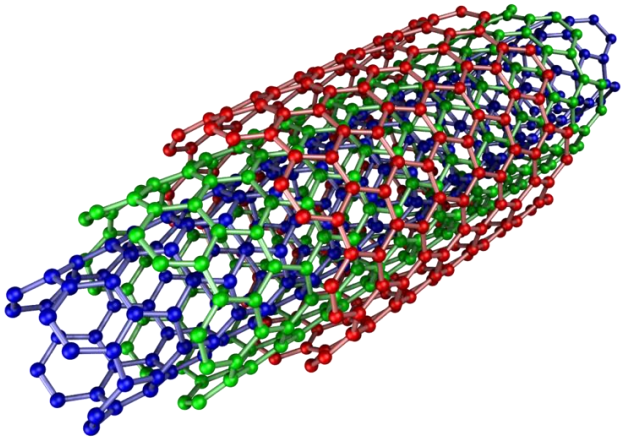

*Figure 1. Structure of multi-walled carbon nanotube.*

Raman spectroscopy is most sensitive to highly symmetric covalent bonds with little or no natural dipole moment. The MWCNTs are made of carbon-carbon covalent bonds, and as a result, Raman spectroscopy is highly sensitive to these materials and able to provide a wealth of information about their structure. Thus, this spectroscopic technique represents a very valuable tool in the characterization of carbon nanomaterials, and specifically carbon nanotubes. [4]

There is a strong correlation between the purity of the MWCNTs and their quality. This is a very important aspect to take into consideration when using them in technological applications. The higher the purity of the nanotubes, the better is their display of properties. In order to evaluate the purity of the carbon nanotubes, the ratio between the intensity of the D and G bands needs to be done. The higher the ratio is, the more disorder is in the material.

## Project goals

The main goal for this project is observing/stating the effect of irradiation with 20 MeV electrons and 1.35 MeV gamma rays on MWCNT, using Raman Spectroscopy measurements taken before and after radiation exposure. Certain objectives need to be set, for this goal to be accomplished. In this case, they around the Raman spectra of the MWCNTs recorded before and after the samples were irradiated. The first objective is to record the Raman spectra, followed by their analysis. The deconvolution of the spectra represents the second objective. Eventually, the analysis and interpretation of the deconvoluted Raman spectra, along with the comparison with the previous results, will provide us with the information needed to complete the study and to draw the conclusions.

This project also presents other adjacent goals, regarding the students who take part in it. Through the objectives previously set, the project aims to provide students with a new set of skills, such as:

- using the OriginPro software for deconvoluting spectra;
- familiarization with the Raman Spectroscopy technique, as well as the properties of MCWNTs and their applications.

All of the steps carried out in this study will help the students complete their knowledge about the use of Raman Spectroscopy applied to the study of radiation damage of MWCNTs, which are of great technological and scientific interest.

## Scope of Work

Radiation effects study on MWCNTs exposed to electron beam and gamma rays using the Raman Spectroscopy is a project meant to find the correlation between the radiation used and the changes that appear in the mullti-walled carbon nanotubes, if any. The practice extended on a 6-week-period of time. The following timeline shows each step taken in order to get closer our goal.

- The first task in aproaching this project was to study the existent literature upon this subject, in order to get acquainted with the topics of Raman Spectroscopy and MWCNTs.
- The next step was the actual experiment: recording the Raman spectra of the MWCNTs both before and after irradiation. The experiment was carried out at Dzhelepov Laboratory of Nuclear Problems (DLNP).
- After the spectra were measured, they were plotted using and compared.
- The last part consisted in the deconvolution of the spectra, followed by their analysis and comparison to the results found previously in the original spectra. The main parameter that was of interest was the ration between the intensity of the G and D peaks, in order to discover any changes in the structure or the quality of the carbon nanotubes.

## Methods

Irradiation with photons of 1.25 MeV ($^{60}$Co) was performed in a therapeutic gamma chamber РОКУЕМ available at the Medical Complex of the DLNP at the Joint Institute for Nuclear Research (JINR). The dose power of the chamber is 148.47 Gy/h. The total exposure dose of the irradiated samples was 23.4 kGy.

*Figure 2. Radiotherapy chamber similar to the one used in the experiment.*


*Figure 3. Position of the chamber head during irradiation.The window in which the samples were directly placed is indicated.*

The photo in *Figure 2* shows the equipment used, and the exposure to radiation was done by rotating the head so that the window was directed upwards and the samples were placed directly on top of it (*Figure 3*). The irradiation time was selected so that the samples received the relevant exposure dose.

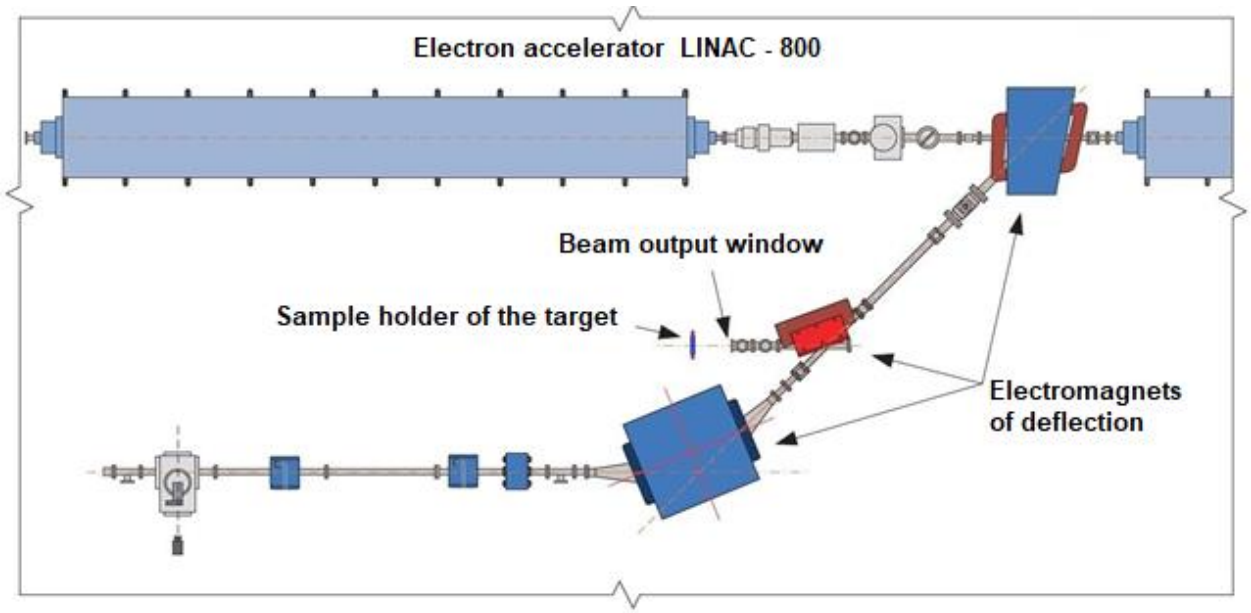


*Figure 4. Overview of the LINAC-800 accelerator and the 20 MeV irradiation station.*

Electron irradiation was performed on the LINAC-800 linear accelerator also of the DLNP –JINR. Its general scheme is presented in *Figure 4*.


*Figure 5. Panoramic view of the LINAC-800 linear accelerator.*

*Figura 6. Irradiation post. A red arrow indicates the exit window and a white arrow indicates the sample holder.*

The picture in *Figure 5* presents a panoramic view of the accelerator (the entire associated technology base of generation, acceleration, vacuum and control are located on the immediate upper floor of the civil construction). The photo in *Figure 6* shows the central beam irradiation station while two of the samples were irradiated.

The samples were placed directly in front of the electron output Ti window, 10 cm from it. It was remotely controlled if they were homogeneously illuminated by the beam throughout the exposure time.

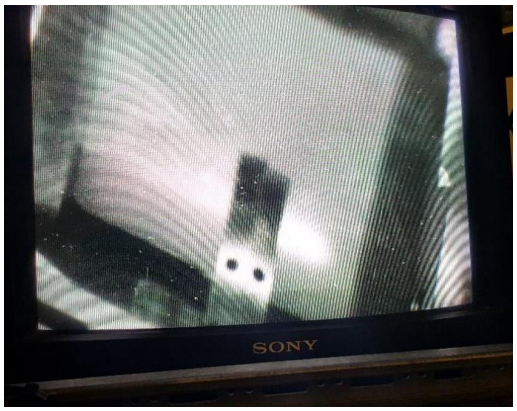


*Figura 7. Real-time image of two of the samples during the irradiation process (black circles at the bottom of the screen).*

*Figure 7* shows the photograph taken by the monitoring camera of the samples in real time while they were being irradiated. The exposed samples (black circles) are visible at the bottom of the monitor screen surrounded by a white halo that is the luminescent emission of the sample holder (beam stain).

The parameters of the beam are presented in *Table I*.

*Table I. The parameters of the beam.*

| | |
|---|---|
| **Energy** | 20 MeV |
| **Current** | 10 mA |
| **Frequency** | 10 Hz |
| **Pulse duration** | 1.5 μs |

Using the corresponding calculations and approximations, it was estimated that the fluence in the sample was $4.38 \times 10^{18}$ $e^{-}$ $cm^{-2}$.

The Raman measurements are done at room temperature in the backscattering geometry [5], using a spectrometer model CARS Solar TII (see *Figure 8*), and applying the following conditions: diffraction grating of 1200 lines/mm, objective 40x (model Olympus-UPlanFL N), and acquisition time 70 s.

*Figure 8. Raman CARS-Solar TII spectrometer.*

The post-processing of the spectra was performed using the software package ORIGIN v.9 [6]. The data obtained from the measurements was normalized and used to plot the spectra. They were plotted on the same graph so the differences that appear after the irradiation can be seen more clearly.

On the other hand, each spectrum underwent the process of deconvolution, in order to find every peak and its intensity. The decomposing of peaks was done using the *Peak Analysis* feature of the OriginPro software.

The Gaussian or Lorentzian functions alone gave unsatisfactory results. Thus, the deconvolution process was carried out using the mathematical function of Voigt that is given by a convolution of a Cauchy-Lorentz distribution and a Gaussian distribution. The definition integral is $V(x;\sigma,\gamma) \equiv \int_{-\infty}^{\infty} G(x';\sigma)L(x-x';\gamma)dx'$, where $G(x';\sigma)\ and\ L(x-x';\gamma)$ are the Gaussian and Lorentz distributions. The defining integral can be evaluated as $V(x;\sigma,\gamma) = \frac{Re[w(z)]}{\sigma\sqrt{2\pi}}$ where Re[w(z)] is the real part of the Faddeeva function evaluated for $z = \frac{x+i\gamma}{\sigma\sqrt{2}}$. By using the Voigt function, we implicitly take into account the two main ways transition lines can be broadened: "homogeneous broadening" (that produce Gaussian line shapes) and "inhomogeneous broadening" (that produce Lorentzian line shapes [7].

# Results and discussion

*Figures 9* and *10* depict the Raman spectra of irradiated and non-irradiated MWCNT in a comparative approach. *Figure 9* illustrates the case where the MWCNT were irradiated with $^{60}$Co photons, while *Figure 10* corresponds to the case where the tubes where irradiated with electrons holding an energy of 20 MeV.

In both images, the main vibrational modes that characterize them have been indicated [8, 9]:

**G** - band peak is assigned to “in plane” displacement of the carbons strongly coupled in the hexagonal sheets. It is associated with an ideal graphitic lattice.

**D** - band is found when disorder is introduced into the graphite structure. D is indicative of the presence of defects in the walls of the tubes. It is associated with a disordered graphitic lattice.

**G$^{I}$** - band is considered a D band overtone (2nd order vibration), also known as 2D. It is associated with the long-range order in a sample mainly along the crystallographic c-axis and provides information on the number of walls. The G$^{I}$ peak arises from the two-phonon second order scattering process, resulting in creation of an inelastic phonon; no defects are required for its activation.

**D+G** - band is related to the combination of phonons with different momenta. Its activation requires a defect. D+G peak strongly supports the presence of higher disorder in the MWCNTs.

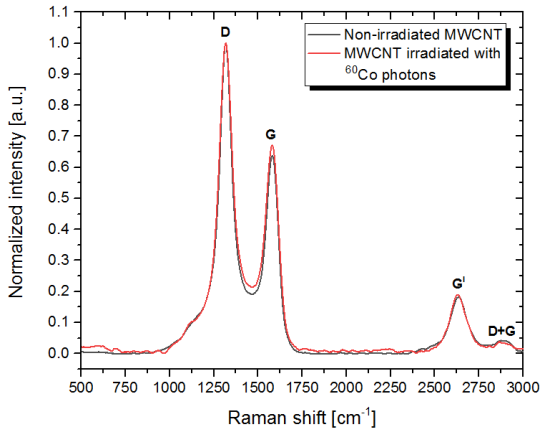


*Figure 9. Raman spectra of MWCNT before and after irradiation with $^{60}$Co photons.*

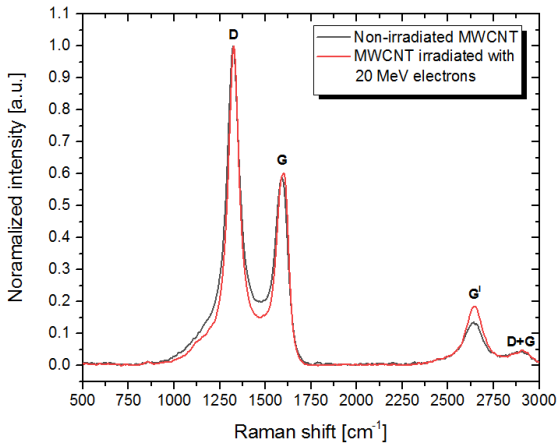


*Figure 10. Raman spectra of MWCNT before and after irradiation with 20 MeV electrons.*

The superposition of the graphs *in Figures 9* and *10* allows the naked eye to establish that, both in the sample irradiated with gamma rays and in the one irradiated with electrons, no significant changes are observed in the position of the fundamental peaks, with respect to the positions of the peaks in the unexposed samples. However, there are perceptible changes in the intensities of the peaks that indicate that structural modifications have taken place in the irradiated samples under the stimulus of the radiation.

In order to determine and quantify these modifications in the spectra more accurately, they were deconvoluted. Decomposing the spectra using the Voigt function gave the best convergence and allowed us to identify the peaks correctly, according to the previous studies done on carbon nanotubes.

*Figures 11* and *12* present each decomposed spectra in the peaks that form it, according to the strategy adopted.

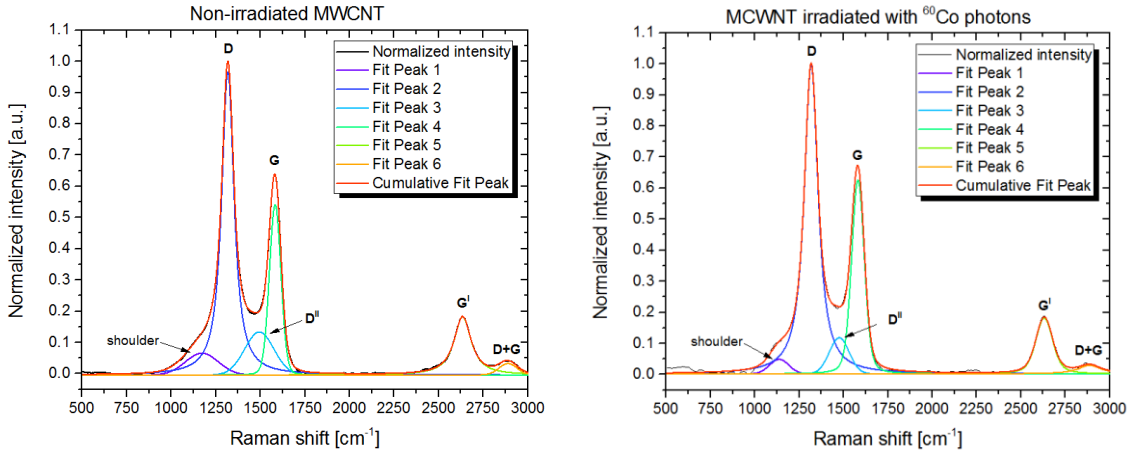


*Figure 11. The deconvoluted Raman spectra of MWCNT with its component peaks, before (a) and after irradiation (b) with $^{60}$Co photons*

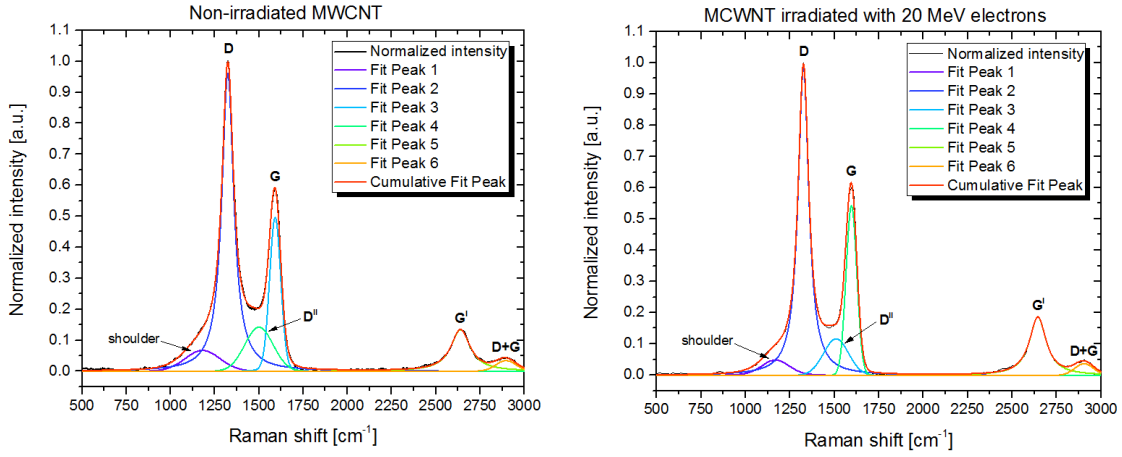


*Figure 12. The deconvoluted Raman spectra of MWCNT with its component peaks, before (a) and after irradiation (b) with 20 MeV electrons*

Visually, the quality of the fit can be said to be good. The data in *Table II*, showing the parameters that evaluate the statistical quality of each fit, corroborates the first impression.

*Table II. Statistical parameters of the fits made in the deconvolution process.*

| MWCNT | Gamma irradiation | | Electron irradiation | |
|---|---|---|---|---|
| | Pristine sample | Irradiated sample | Pristine sample | Irradiated sample |
| Reduced Chi-sqr ($\chi^2$) | 7.017E-6 | 3.393E-5 | 1.127E-5 | 1.693E-5 |
| R-sqr ($R^2$) | 0.99977 | 0.99903 | 0.99962 | 0.99968 |

In these graphs, in addition to the previously identified modes, it has now been possible to establish the presence of two other peaks.

**$D^{II}$** - band reported to be associated with amorphous $sp2$-bonded forms of carbon.

**Low frequency shoulder** – its origin has not been clearly identified. Probably the shoulder has its origin in double resonance process, because its Raman shift (~1200 $cm^{-1}$) is a point on phonon dispersion [10].

*Table III* presents the intensities of the main vibrational modes (D and G) and the relationship between them to illustrate the analysis that will be done below. Changes in intensities can be seen in all modes after the samples were exposed to radiation.

*Table III. Values of the intensities of the main modes of the spectra under study.*

| MWCNT | Gamma irradiation | | Electron irradiation | |
|---|---|---|---|---|
| | Pristine sample | Irradiated sample | Pristine sample | Irradiated sample |
| D mode intensity [a.u.] | 0.966 | 0.997 | 0.961 | 0.985 |
| G mode intensity [a.u.] | 0.541 | 0.625 | 0.495 | 0.542 |
| ID/IG | 1.787 | 1.594 | 1.941 | 1.818 |

As can be seen in *Figures 11 and 12,* and in *Table III*, the D band in all cases is more intense than the G band, which reveals the presence of structural defects in the carbon nanotubes, a consequence of the particular characteristics of MWCNTs due to their multiple graphite layers.

The intensities ratio ID/IG is known to be directly proportional to graphitization of carbon materials. Thus, this value allows the characterization of the disorder level of CNT samples [11].

As can be seen in *Table III*, the ID/IG ratio of the pristine samples was higher than the irradiated ones, which may indicate that the structural defects of the multilayer nanotubes decreased under the action of radiation.

For the case of the sample exposed to gamma rays, the ID/IG analysis in the studied samples showed that apparently the gamma irradiation process improved the degree of structural order in the graphite layers. In other words, the $^{60}$Co gamma radiation at the studied dose induced a decrease in the structural defects of the nanotubes.

This process is possible considering that at relatively low gamma doses the crystal lattice can be favored with a process of rearrangement or relaxation of the remaining primary structural effects (annealing stimulated by gamma rays) [12, 13].

In the samples that were exposed to the 20 MeV electrons, the obtained spectra (*Figure 12a*) showed a slightly different behavior than the one manifested after irradiation with gamma rays.

Note that the ID/IG variation is small in favor of the quality of the MWCNTs (although it exists), however, it can be seen that the intensity of the $G^{I}$ band increased significantly with respect to that of the non-irradiated sample. Certainly $G^{I}$ is also used to evaluate the quality of the structure of the nanotube material, and authors such as [11, 14] emphasize that it is a better indicator of the crystallinity of the material, therefore, its increase with respect to D or G may be an indication of the decrease in the number of defects.

It is important to highlight that the intensity of the $G^{I}$ band is strongly related to the number of layers of the tube, being used precisely for the purpose of its determination [15]. That is why it could be thought that the electrons in this experiment, in addition to slightly improving the quality of the irradiated multilayer material, are actively participating in its exfoliation.

We are not going to analyze the behavior of the D + G band, because according to reports in the literature, it provides similar information as the D band [10].

# Conclusions

Multi-walled carbon nanotubes have a particular structure that makes them very useful in many fields of scientific research and practical applications. For this reason, the study of radiation damage is very important, since this material can be used in radiation-aggressive media that can modify its structure and properties. In this study, Raman spectroscopy has been used to analyze the target samples before and after being exposed to two different sources of radiation: gamma rays of 1.25 MeV and electrons accelerated up to 20 MeV. The intercomparison of the simple spectra showed that there were no significant shifts of the peaks, but there were changes in their intensities after the samples were irradiated, indicating that structural changes have taken place. The deconvolution of the spectra carried out by applying the Voigt function allowed obtaining the information of all the peaks present and making the comparison between the different vibrational modes more precise. The analysis of the results indicates that both the $^{60}$Co gamma photons and the 20 MeV electrons positively influence the structure of the target MWCNTs, favoring the increase in the crystallinity of the material as a result of the reduction of defects. Evidence was also found that electron irradiation has an exfoliating effect on the multilayer structure of the samples.

As a recommendation of this work, in order to reach firmer conclusions, it is proposed to carry out a more detailed analysis of the structure of the D, G and G' modes, and of other peaks that appear in the deconvoluted spectra, and to delve into the study of its evolution with the exposure dose and the characteristics of the source.

# Acknowledgements

I would like to thank the Joint Institute of Nuclear Research for making the "International Remote Student Training". This INTEREST program has allowed me in only a month and a half to get new knowledge about the multi-walled carbon nanotubes, the spectroscopic technique based on the Raman Effect and its use to study the radiation damage in materials, the deconvolution procedures for spectra analysis, the different irradiation facilities existing in the JINR, particularly in the DLNP, etc.

# References


[1] Gardiner D. J. Practical Raman spectroscopy. Springer-Verlag (1989).

[2] Chakrapani N., Curran S., Bingqing W., *et al*. Spectral fingerprinting of structural defects in plasma-treated carbon nanotubes. J. Mater. Res. 18(10) (2003) 2515-2521.

[3] S. Das. A review on Carbon nano-tubes – A new era of nanotechnology. International Journal of Emerging Technology and Advanced Engineering. 3(3) (2003) 776.

[4] J. Hodkiewicz. Characterizing Carbon Materials with Raman Spectroscopy, Thermo Fisher Scientific Inc., Madison, WI, USA. Application Note: 51901, (2010).

[5] J. Ferraro, K. Nakamoto and Ch. W. Brown. Introductory Raman Spectroscopy, Chap. 2 - Instrumentation and Experimental Techniques, 2nd Edition, Academic Press, (Amsterdam, 2003).

[6] Origin v.9.0., OriginLab Corporation, (Northampton, MA, 2012).

[7] B.H. Armstrong. Spectrum line profiles: The Voigt function. Journal of Quantitative Spectroscopy and Radiative Transfer, 7(1) (1967) 66-68

[8] M. S. Dresselhaus, G. Dresselhaus, R. Saito and A. Jorio. Raman spectroscopy of carbon nanotubes. Physics Reports 409 (2005) 47–99.

[9] E. I. Bîru and H. Iovu. Graphene Nanocomposites Studied by Raman Spectroscopy, Raman Spectroscopy, Gustavo Morari do Nascimento, IntechOpen (2018) 192

[10] E. F. Antunes, A. O. Lobo, E. J. Corat, *et al.* Comparative study of first- and second-order Raman spectra of MWCNT at visible and infrared laser excitation. Carbon 44 (2006) 2202–2211.

[11] R. A. DiLeo, B. J. Landi, and R. P. Raffaelle. Purity assessment of multiwalled carbon nanotubes by Raman spectroscopy. Journal of Applied Physics, 101(6) (2007) 064307.

[12] X. Zhiwei, Ch. Lei, L. Liangsen, *et al.* Structural changes in multi-walled carbon nanotubes caused by γ-ray irradiation. Carbon 49(1) (2011) 339-351.

[13] B. Safibonaba, A. Reyhani, A. N. Golikand, *et al.* Improving the surface properties of multi-walled carbon nanotubes after irradiation with gamma rays Applied Surface Science 258(2) (2011) 766-773.

[14] E. Dervishi, Z. Li, F. Watanabe, *et al.* Thermally controlled synthesis of single-wall carbon nanotubes with selective diameters. J. Mater. Chem. 19 (2009) 3004-3012.

[15] Gayathri S., Jayabal P., Kottaisamy M., and Ramakrishnan V. Synthesis of few layer graphene by direct exfoliation of graphite and a Raman spectroscopic study. AIP Advances 4 (2014) 027116.